

Adsorption Equilibrium Characteristics of Phenol and Lead on Bamboo Chitosan Composite Bead

Dong Seon Kim, Byoung Jun Min, Pan Pan Sun, Sung Yong Cho, and Tae Young Kim*

Department of Environmental Energy Engineering, Chonnam National University, Gwangju, 61186, Korea
Email: gosto1004@jnu.ac.kr (D.S.K.); syc@jnu.ac.kr (S.Y.C.); tykim001@chonnam.ac.kr (T.Y.K.)

*Corresponding author

Manuscript received January 14, 2022; revised February 25, 2024; accepted March 3, 2024; published April 16, 2024

Abstract—The adsorption equilibrium characteristics for single and binary components of phenol and lead ions on Bamboo Chitosan Composite Bead (BCB) were studied. The surface areas of BCB beads increased with the increasing amount of Bamboo Activated Carbon (BAC) contained. Adsorption equilibrium data for the single component of phenol and lead ions on the adsorbents could be represented by the Langmuir equation. The maximum adsorption amount of lead ions on chitosan bead was 0.85 mol/kg. Multicomponent equilibrium data were correlated by the extended Langmuir and Ideal Adsorbed Solution Theory (IAST). The IAST gave the best fit to our data. The adsorption capacity of lead ions on the different adsorbents was in the following order: chitosan (0.85) > BCB-1 (0.49) > BCB-2 (0.23) > BAC (0.2 mol/kg). On the other hand, that of phenol was: BAC (1.81) > BCB-2 (0.93) > BCB-1 (0.61) > chitosan (0.03 mol/kg).

Keywords—adsorption, bamboo, chitosan, lead, phenol

I. INTRODUCTION

In recent years, water pollution has become increasingly serious. Phenolic compounds and heavy metals are common pollutants in stream water, and because of their toxicity, carcinogenicity, and accumulation in the food chain, pose a potential threat to the ecosystem [1–3]. Furthermore, these compounds may occur together in contaminated water, with their combined toxicity and relative mobility giving rise to more serious damage to the environment [4–6]. Lead ions may affect the brain and nervous system development in children, and cause high blood pressure, kidney damage, and miscarriage in adults. Phenol may also contribute to nausea and skin corrosion. Because of the severe consequences of water pollution, efficient pollutant removal techniques are being developed. Conventional treatment technologies for the removal of heavy metals and organic compounds have been extensively investigated, such as adsorption, ion exchange, photocatalysis techniques, and nanofiltration [7, 8].

Chitosan, [β -(1-4)-2-amino-2-deoxy-D-glucopyranose], is produced by the partial alkaline N-deacetylation of chitin, which can be widely found in the exoskeleton of shellfish and crustaceans as the second most abundant natural biopolymer next to cellulose. It has been used in several applications of water purification [9], drug delivery [10], cosmetics [11] and coating [12], using forms such as membranes, beads, capsules, gels, and fibers. It is known as an outstanding adsorbent with extremely high and selective affinity for heavy metal ions, because the amine, amide, and hydroxyl groups on chitosan chains serve as coordination sites, and because of its environment friendliness.

Bamboo is a tropical plant, and is common in East and Southeast Asia, such as China, Thailand, Vietnam, and Korea. Bamboo Based Activated Carbon (BAC) constitute an environment friendly, biodegradable, low-cost, and renewable bioresource with porous materials. BAC can be expected to be used as a potential commercially available activated carbon for the treatment of gaseous pollutants in industrial effluents and liquid pollutants in drinking water filtration applications [13–15].

In this study, porous chitosan bead was obtained by sol-gel method. BAC was prepared by KOH activation, and to achieve high application potential for the chitosan bead, chitosan bead containing bamboo activated carbon (BCB-1 and BCB-2) was developed. The purpose of this article, investigate the adsorption of chitosan, Bamboo Chitosan Composite Bead (BCB), BAC in the removal of lead ions and phenol of single and binary solution. The surface area, pore volume and pore morphology of chitosan bead, BCB and BAC were characterized by Brunauer–Emmett–Teller (BET) and Scanning Electron Microscope (SEM).

II. ISOTHERM MODELING

A. Single-Species Isotherm

Adsorption phenomenon mechanisms are so complicated that no simple theory can adequately explain adsorption equilibrium characteristics. Many expressions have been reported that describe the adsorption equilibrium relationship between the adsorbate and the adsorbent. The Langmuir, Freundlich, and Sips isotherm models were fitted to describe the equilibrium adsorption. These equations of isotherms are given below:

$$\text{Langmuir isotherm, } q = \frac{q_m k_L C_e}{1 + k_L C_e} \quad (1)$$

where, C_e is the supernatant concentration at the equilibrium state of the system (mol/m³), k_L is the Langmuir affinity constant (m³/mol), and q_m is the maximum adsorption capacity of the material (mol/kg), assuming a monolayer of adsorbate uptaken by the adsorbent.

$$\text{Freundlich isotherm, } q = k_F C_e^{1/n} \quad (2)$$

where, k_F is the Freundlich constant related to adsorption capacity (mol/kg) (mol/m³)^{-1/n}, and n is the Freundlich exponent (dimensionless).

$$\text{Sips isotherm, } q = \frac{q_m k_s C_e^{1/n}}{1 + k_s C_e^{1/n}} \quad (3)$$

where, k_s is the Sips constant related to the affinity constant $(\text{mol/m}^3)^{-1/n}$, and q_m is the Sips maximum adsorption capacity (mol/kg).

B. Multi-Species Isotherm

When two or more components exist with the possibility of occupying the same adsorption sites, equilibrium relationships become more complex. The simplest is the extension of the Langmuir isotherm by assuming no interaction between adsorbing molecules. This equation enables quick estimation of the equilibrium relations of multi-species adsorption from the Langmuir parameters determined from the single-species isotherm of each component. The extended Langmuir equations are as follow:

$$q_i = \frac{q_m b_i C_i}{1 + \sum_j b_j C_j} \quad (4)$$

One of the most widely used thermodynamic models is the ideal Adsorbed Solution Theory (IAST). IAST theory has been reported to predict the multi-component adsorption systems successfully using only pure component experimental data. This theory has been developed by Myers and Prausnitz and widely utilized in the literature to predict equilibrium adsorptive properties of different adsorbents [16, 17].

C. Preparation of the Porous Chitosan Bead and Bamboo Chitosan Composite Bead (BCB) Beads

Flake form of chitosan was purchased from Sehwa Co., Korea, and used without further purification. The flaked form of chitosan was milled by ball mill to pass through a 125 μm sieve. The degree of deacetylation of chitosan powder was determined to be 85 %. The chitosan powder has low porosity, low specific surface area, and low resistance to mass transfer. To overcome these disadvantages, porous chitosan bead was obtained by the sol-gel method. The chitosan powder was dissolved in 3 wt.% CH_3COOH solution to produce a viscous solution with approximately 5 wt.% chitosan. The viscous chitosan solution was then dropped into chitosan beads by a phase-inversion technique using 2 M NaOH solution at 298 K. The chitosan droplets formed beads in the NaOH solution, and were left in the gelation agent solution for overnight. The reaction of CH_3COOH with NaOH solution caused the precipitation of the chitosan droplets. Thereby, uniformly spherical chitosan gel beads were formed. BCB-1 and BCB-2 beads were prepared by mixing 1 and 2 g of BAC, respectively, with 100 mL of 5 wt.% chitosan solution, in the same manner as in the preparation of the chitosan bead. The chitosan, BCB-1, and BCB-2 beads were thoroughly washed with deionized water to removal excessive sodium hydroxide inside the beads, and stored in distilled water, until use.

D. Preparation of the Bamboo Activated Carbon

The bamboo was obtained at Damyang (Korea), and cut into particle size in the range 2–3 mm to prepare bamboo chips. In the activation process, the bamboo chips were impregnated in 50 wt.% KOH solution for 3 days (d), and then dried at 105 $^\circ\text{C}$ for 2 d. The obtained material was placed in a furnace, followed by heating to the carbonization temperature of 450 $^\circ\text{C}$ at an increasing rate of 5 $^\circ\text{C}/\text{min}$, and

maintained at that temperature for 0.5 h under N_2 atmosphere. The material was then heated to activation temperature of 750 $^\circ\text{C}$, and maintained at that temperature for 1 h. The obtained BAC was washed with deionized water, until the pH was neutral. Finally, the BAC was dried in oven at 105 $^\circ\text{C}$ for 24 h.

E. Isotherm Test

Adsorption equilibrium isotherms for single and binary components of lead ions and phenol on various natural adsorbents were determined by contacting a volume of the solutions with a carefully weighted amount of BAC, chitosan bead, BCB-1 and BCB-2 beads in a conical flask, respectively. The amounts of the adsorbents were varied (0.001–0.5) g, and the volume of lead ions and phenol solution was 100 mL of 1.06 mol/m³. HCl and NaOH solutions were used to adjust pH of the solution. The conical flasks were shaken for 2 d to provide sufficient time and contact for equilibrium between the adsorbents and adsorbates. Prior to analysis of the samples taken from the conical flask, they were filtered to remove suspended powdered BAC particles.

The concentrations of lead ions and phenol were determined by ICP (Shimadzu) and UV-spectrophotometry (Shimadzu 1601) at $\lambda = 284$ nm, respectively.

The amount of lead ions and phenol adsorbed at equilibrium were calculated from the following mass balance equation as:

$$q = \frac{(C_i - C_e)V}{W} \quad (5)$$

where, q is the equilibrium amount adsorbed by the adsorbents (mol/kg), C_i is the initial concentration of bulk fluid (mol/m³), C_e is the equilibrium concentration of the solution (mol/m³), V is the volume of solution (m³), and W is the weight of the adsorbent (kg).

III. RESULTS AND DISCUSSION

A. Characterization of the Adsorbents

The heat of carbonization of bamboo must be determined to calculate the material balance for the bamboo carbonization process. The heat of carbonization can be found by using a Thermo-Gravimetric Analysis (TGA) curve and differential thermos-gram (DTG) of the bamboo acquired using a TGA/DTA analyzer (SEIKO SII, Japan). Fig. 1 is a TGA and DTG curves obtained by heating the bamboo at a heating rate of 10 $^\circ\text{C}/\text{min}$ in a flowing stream of helium. As can be seen in the figure, the thermal decomposition of bamboo occurred in two stages. The first stage occurred between 0 $^\circ\text{C}$ and 200 $^\circ\text{C}$, and the weight loss in this stage was about 8.88%. The second stage occurred between 240 $^\circ\text{C}$ and 350 $^\circ\text{C}$, and this stage was about 63.95%. Shao *et al.* [18] reported that the first stage was the drying and dehydration stage; the weightlessness was mainly affected by the moisture content of the sample. The second stage of weight loss was caused by the volatilisation of small molecular gases, such as the volatilisation of CO_2 produced by the cleavage reaction of C=C or C=O bonds. In this study, the Scanning Electron Microscope (SEM) was used to pore morphology for BAC, chitosan bead, BCB-1 bead, and BCB-2 bead.

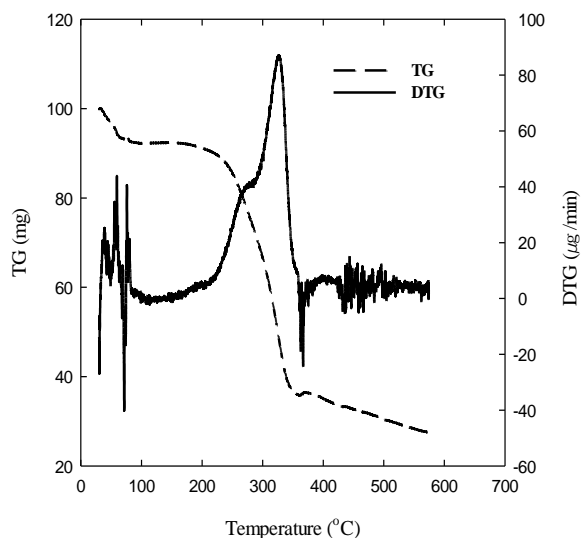
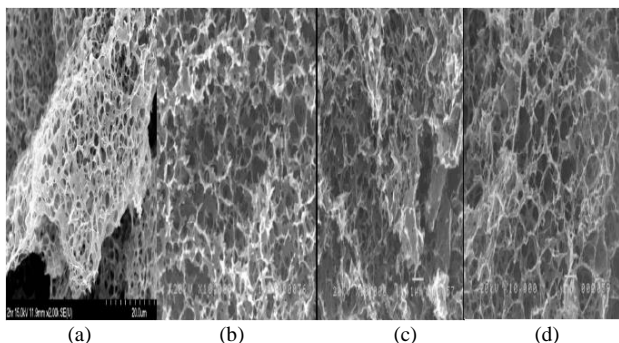


Fig. 1. Thermogram for the carbonization of a bamboo.


 Fig. 2. SEM photography of (a) BAC, (b) chitosan bead, (c) BCB-1 bead, and (d) BCB-2 bead ($\times 10,000$).

The porous structure of (a) BAC (b) chitosan bead, (c) BCB-1 bead, and (d) BCB-2 bead can clearly be seen in Fig. 2. The highly reticular, three dimensional porous matrix of BAC, chitosan bead, BCB-1 and BCB-2 bead cross section are particularly evident at $\times 10,000$. In case of BAC, the pore structure was developed during the activation process, high temperature pyrolysis removed tar and organic substances. The water vapor activator diffuses into the interior of BAC, reacted with the carbon and formed the pore structure of the carbon material. When the lignin and cellulose were completely carbonized, the pore structure and pore channels become more and more clear [18]. The uniform pore structure distribution of BAC, chitosan bead, BCB-1 and BCB-2 bead is an important criterion for adsorption of lead ions and phenol on the whole surface area of the adsorbents. The specific surface area of the BAC, chitosan bead, BCB-1 and BCB-2 bead were measured from N_2 adsorption/desorption isotherm at 77 K (Quantachrome, USA). The mean diameter of chitosan bead, BCB-1 and BCB-2 bead was 2 mm. The specific surface area and micro pore volume of BAC calculated from Fig. 3 and the values were 1,634 m^2/g and 0.36 cc/g respectively. After being modified by chitosan (315 m^2/g and 0.8 cc/g), the specific surface area of BCB-1 bead and BCB-2 bead was decreased to 516 and 640 m^2/g , and the micro pore volume is increased to 0.40 and 0.39 cc/g . The above results indicated that adsorption of phenol and lead ions on bamboo chitosan composite bead was not only related to the specific surface

area and pore volume but also may depend on surface properties of BAC and chitosan. The physical properties of the adsorbents used in this study are summarized in Table 1.

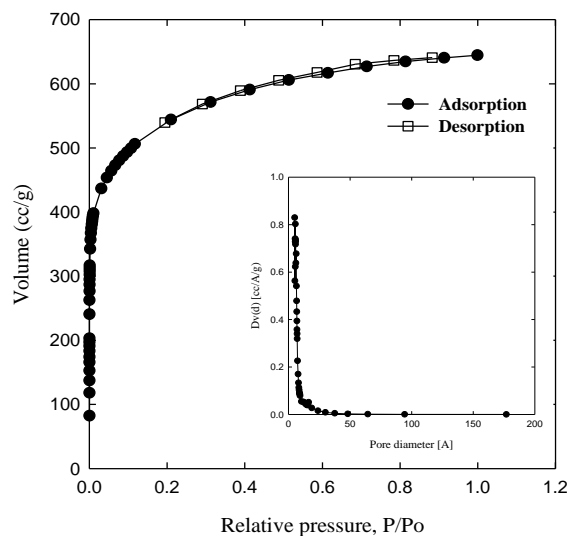


Fig. 3. Adsorption/desorption isotherm and pore size distribution of BAC.

Table 1. Physical properties of the adsorbents used in this study

Properties	BAC	Chitosan	BCB-1	BCB-2
Chitosan/BAC ratio	0/1	1/0	1/0.5	1/1
Mean diameter [mm]	0.04	2.0	2.0	2.0
BET surface area [m^2/g]	1,634	315	516	640
Pore volume [cm^3/g]	0.36	0.8	0.40	0.39

B. Adsorption Equilibrium

Fig. 4 shows the adsorption amount of lead ions on the four different adsorbents at 298 K and pH 5.1. The adsorption amounts of lead ions on chitosan bead (0.85 mol/kg) was greater than that on BAC (0.20 mol/kg). In the case of chitosan bead, the excellent adsorption of lead ions was most likely due to its high hydrophilicity, caused by its large number of hydroxyl groups and primary amino groups with high activity as adsorption sites. This high density of free amino groups allows the chitosan to interact as a primary amine with the heavy metal. The adsorption capacities of lead ions on four different adsorbents were in the following order: chitosan bead > BCB-1 bead > BCB-2 bead > BAC. On the other hand, the adsorption amount of lead ions on BCB-1 bead (0.49 mol/kg) was greater than that on BCB-2 bead (0.23 mol/kg). Since BCB-1 bead contained more chitosan than BCB-2 bead. It is well known that the adsorption amount of commercial activated carbon for heavy metals is very little compared to natural polymer or ion exchange resin [19–20]. In this study, three isotherm models, the Langmuir, Freundlich, and Sips, were used to correlate our experimental adsorption equilibrium data on the adsorbents for lead ions and phenol. To find the parameters for each adsorption isotherm, the linear least square method and the pattern search algorithm were used. The value of the mean percentage error has been used as a test criterion for the fit of the correlations. The mean percent deviation between the experimental and predicted values was obtained using Eq. (6):

$$error(\%) = \frac{100}{N} \sum_{k=1}^N \left[\frac{|q_{exp,k} - q_{mol,k}|}{q_{exp,k}} \right] \quad (6)$$

where, $q_{model,k}$ is each value of q predicted by the fitted model, $q_{experimental,k}$ is each value of q measured experimentally, and N is the number of experiments performed.

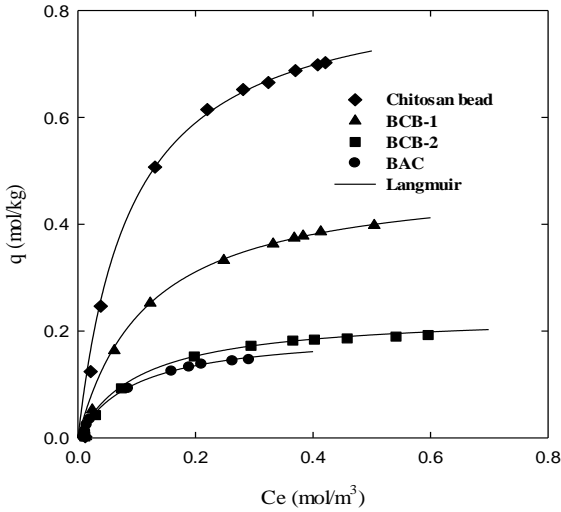


Fig. 4. Adsorption isotherms of lead ions on different adsorbents (pH: 5.1, 298 K).

Table 2. Adsorption equilibrium constants of Pb²⁺ and phenol on different adsorbents (298 K, pH 5.1)

	Isotherm	Parameters	BAC	Chitosan	BCB-1	BCB-2
Pb ²⁺	Langmuir	q_m	0.20	0.85	0.49	0.23
		b	10.40	11.15	8.53	9.57
		error (%)	0.11	0.34	0.14	0.32
	Freundlich	k	0.35	0.93	0.53	0.23
		n	1.67	3.34	2.78	3.66
		error (%)	1.91	0.95	0.32	0.76
	Sips	q_m	0.20	0.85	0.49	0.23
		b	10.37	11.33	8.48	9.82
		n	1.00	0.99	1.00	0.99
		error (%)	1.02	0.37	0.15	0.34
phenol	Langmuir	q_m	1.81	0.03	0.61	0.93
		b	18.20	6.59	10.42	8.39
		error (%)	0.05	0.05	0.03	0.03
	Freundlich	k	1.72	0.03	0.56	0.83
		n	8.75	6.78	10.97	6.40
		error (%)	1.03	0.09	0.06	0.36
	Sips	q_m	1.81	0.03	0.61	0.93
		b	18.42	6.53	10.44	8.42
		n	0.99	1.00	0.99	0.99
		error (%)	0.06	0.05	0.03	0.03

The parameters and the average percent differences between measured and calculated values for lead ions on the different adsorbents are given in Table 2. As shown in the table, the Langmuir equation gives the best fit of our data among the three.

Fig. 5 shows the adsorption capacity of phenol on the four different adsorbents at 298 K and pH 5.1. The adsorption amounts of phenol on BAC (1.81 mol/kg) was much higher

than that on chitosan bead (0.03 mol/kg). On the other hand, the adsorption amount of phenol on BCB-2 bead (0.93 mol/kg) was greater than that on BCB-1 bead (0.61 mol/kg). Because the specific surface area of BCB-2 bead (640 m²/g) was larger than that of BCB-1 bead (516 m²/g). The adsorption amounts of phenol on the four different adsorbents were in the following order: BAC > BCB-2 bead > BCB-1 bead > chitosan bead. Compared to Figs. 4 and 5, the natural polymer is an excellent adsorbent for the heavy metal, and BAC is for the organic. However, BCB beads could be used for the simultaneous removal of lead ions and phenol. Since the beads possess the advantage of chitosan and BAC adsorbent. The parameters and the average percent differences between measured and calculated values for phenol on the different adsorbents are given in Table 2. Based on the error, the Langmuir model was the best isotherm model for the adsorbents. The Langmuir model showed the lowest error values, which means that the q fit by the isotherm model was close to the q measured experimentally. However, the Freundlich and Sips isotherm models also simulated well the adsorption data for phenol on the adsorbents.

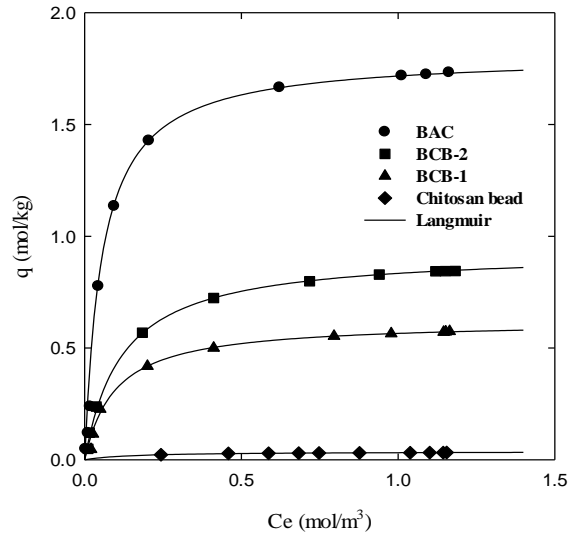


Fig. 5. Adsorption isotherms of phenol on different adsorbents (pH: 5.1, 298 K).

The effect of pH on adsorption capacity of phenol on BCB-2 bead was evaluated from the measurement of the adsorption equilibrium data at 298K. As shown in Fig. 6, adsorption capacity of phenol on BCB-2 bead increased with decreasing initial pH of the solution. This phenomenon can be attributed to the fact that a lower pH increases the positively charged groups on the surface of BCB-2 bead, and the surface charges on the adsorbate in value higher than pK_a (9.89 for phenol) are mostly anionic. On the other hand, in the basic condition, the surface functional groups of BCB-2 bead, such as carboxylic, hydroxyl, and amine, are very weak, so that repulsion between the surface layer and the anionic phenol results in reduced adsorption. Garcia et al. reported that below the pHPZC of granular activated carbon, the surface charge of granular activated carbon was predominantly positive, having a higher affinity for anions [21]. The estimated values of the adsorption equilibrium parameters are summarized in Table 3. As can be seen in this table, the maximum adsorption amount of phenol on BCB-2 bead at pH

5.1, 7 and 10 was 0.93, 0.88, and 0.81 mol/kg, respectively.

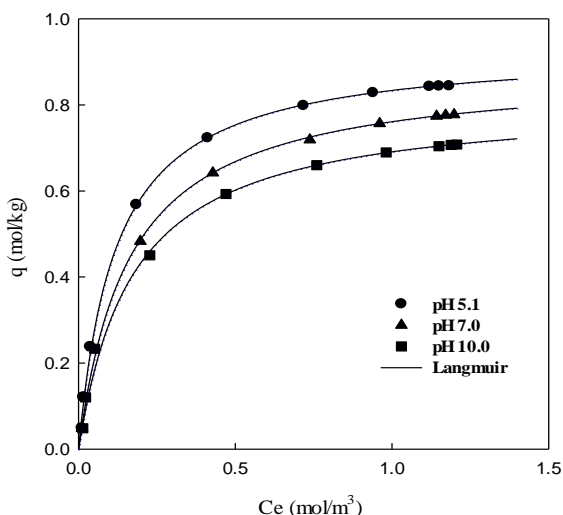


Fig. 6. Adsorption isotherms of phenol on BCB-2 bead in terms of the initial pH.

Table 3. Adsorption equilibrium constants of phenol on BCB-2 bead in terms of pH (298 K)

Isotherm	Parameters	pH 5.1	pH 7.0	pH 10.0
Langmuir	q_m	0.93	0.88	0.81
	b	8.39	6.21	5.77
	error (%)	0.03	0.02	0.06
Freundlich	k	0.83	0.75	0.69
	n	6.40	5.14	6.34
	error (%)	0.36	0.41	0.17
Sips	q_m	0.93	0.88	0.80
	b	8.42	6.22	5.81
	n	0.99	0.99	0.99
	error (%)	0.03	0.02	0.06

In binary adsorption systems, the equilibrium uptakes of phenol and lead ions on the BCB-1 and BCB-2 beads were predicted, and compared with the experimental amounts adsorbed. Multi-species adsorption isotherms, such as the extended Langmuir and Ideal Adsorbed Solution Theory (IAST) were used to predict those binary data. The binary experiments for phenol and lead ions systems on BCB-1 and BCB-2 beads were performed under the conditions (C_0 : 0.106 mol/m³, contact time: 48 h, temperature: 298 K). For multi-component systems, the adsorbent and adsorbate affinity will change, due to the competition for available adsorption sites. It can be seen in Fig. 7, the maximum adsorbed amount of phenol and lead ions in binary solutions on BCB-1 bead was 0.85 and 0.60 mol/kg, respectively. In the case of phenol, the predicted maximum adsorbed amount for the extended Langmuir and IAST theory were 0.87 and 0.61 mol/kg, respectively. On the other hand, the predicted maximum adsorbed amount of lead ions for the extended Langmuir and IAST theory were 0.57 and 0.47 mol/kg, respectively. The amount of phenol adsorbed on BCB-1 bead was higher than that of lead ions. As can be seen in Figs. 4 and 5, the adsorption amount of phenol (0.61 mol/kg) on BCB-1 was greater than that of lead ions (0.49 mol/kg). When adsorption competes in a binary system, the high adsorption affinity molecule (phenol) will occupy the pores first (BCB-1). Basically, if most of the data are distributed around the 45° line (see Fig. 7), this indicates that the models

suitably represent the experimental data of the system. However, the extended Langmuir model gave considerable deviation between the calculated and predicted amounts in the phenol and lead ions systems. But the IAST gave the best fit to all data in the binary systems. The IAST may be a favorable theory adaptable to the removal of phenol and lead ions of binary systems using BCB-1 bead.

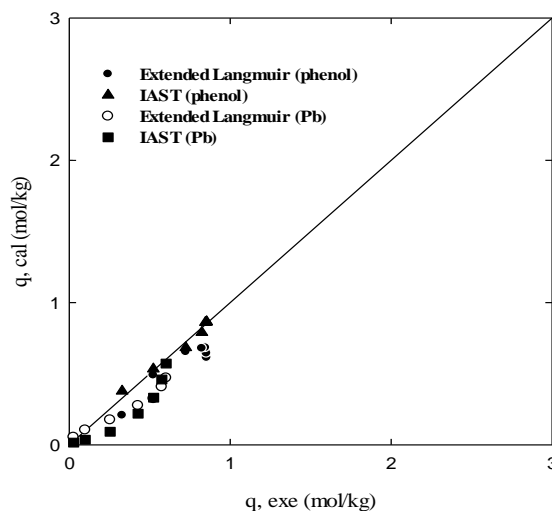


Fig. 7. Measured and predicted adsorption uptakes of lead ions and phenol on BCB-1 bead in the binary components.

The adsorption equilibrium amounts for binary components of lead ions and phenol on BCB-2 beads were shown in Fig. 8. The maximum adsorbed amount of lead ions and phenol in binary solutions on BCB-2 bead was 0.41 and 1.13 mol/kg, respectively. In case of phenol, the predicted adsorption amounts for extended Langmuir and IAST theory was 1.13 and 1.03 mol/kg, respectively. Compared to Figs. 4 and 5, the natural polymer is an excellent adsorbent for the heavy metal and BAC is for the organic. However, BCB beads could be used for simultaneous removal of lead ions and phenol. Since the beads possess the advantage of chitosan and BAC adsorbent. Compared with Figs. 7 and 8 in binary system, the amount of phenol adsorption was high on BCB-2 bead containing a lot of BAC. Conversely, BCB-1 bead with high chitosan content was high adsorption amount of lead ions.

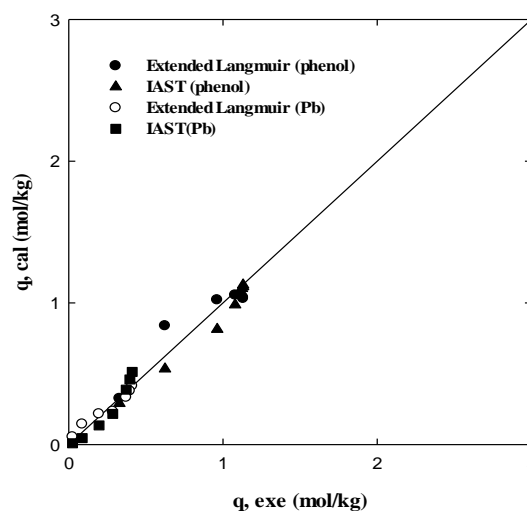


Fig. 8. Measured and predicted adsorption uptakes of lead ions and phenol on BCB-2 bead in the binary components.

IV. CONCLUSIONS

The specific surface area of chitosan bead, BCB-1, BCB-2, BAC was 315, 516, 640, and 1,634 m²/g. Adsorption equilibrium data for single component of lead ions and phenol on the different adsorbents could be represented by the Langmuir equation. The adsorption capacity for single component of lead ions on the different adsorbents was in the following order: chitosan bead (0.85) > BCB-1 (0.49) > BCB-2 (0.23) > BAC (0.20 mol/kg). On the other hand, that of phenol was: BAC (1.81) > BCB-2 (0.93) > BCB-1 (0.61) > chitosan bead (0.03 mol/kg). Adsorption equilibrium data for multicomponent of lead ions and phenol could be represented by IAST. The adsorption amount of phenol on BCB beads in the binary component was greater than that of lead ions.

CONFLICT OF INTEREST

The authors declare no conflict of interest.

AUTHOR CONTRIBUTIONS

The first author conducted the research and data analysis; The corresponding author wrote the paper; The other authors provided assistance throughout all stages of the work; all authors had approved the final version.

FUNDING

This work was supported by Korea Institute for Advancement of Technology. Also, supported by Gwangju Green Environment Center as “Research Development Project (21-04-40-43-12)”.

REFERENCES

- [1] L. M. Huong, D. B. Thinh, T. H. Tu, N. M. Dat, T. T. Hong, P. T. N. Cam, D. N. Trinh, H. M. Nam, M. T. Phong, and N. H. Hieu, “Ice segregation induced self-assembly of graphene oxide into graphene-based aerogel for enhanced adsorption of heavy metal ions and phenolic compounds in aqueous media,” *Surf. Interfaces.*, vol. 26, 101309, Oct. 2021.
- [2] M. H. Wang, L. L. Yan, S. Dou, L. Yang, Y. Zhang, W. H. Huang, S. S. Li, P. Lu, and Y. M. Guo, “Blood multiple heavy metals exposure and lung function in young adults: A prospective Cohort study in China,” *J. Hazard. Mater.*, vol. 459, 132064, 2023.
- [3] L. G. Ma, Y. C. Zhou, A. Wang, and Q. L. Li, “A potential heavy metals detoxification system in composting: Biotic and abiotic synergy mediated by shell powder,” *Bioresour. Technol.*, vol. 386, 129576, 2023.
- [4] Y. Li, H. Y. Bi, X. M. Mao, Y. Q. Liang, and H. Li, “Adsorption behavior and mechanism of core-shell magnetic rhamnolipid-layered double hydroxide nanohybrid for phenolic compounds from heavy metal-phenolic pollutants,” *Appl. Clay Sci.*, vol. 162, pp. 230–238, Sep. 2018.
- [5] S. Chen, R. Lin, H. Lu, Q. Wang, J. J. Yang, J. C. Liu, and C. Yan, “Effects of phenolic acids on free radical scavenging and heavy metal bioavailability in *kandelia obovata* under cadmium and zinc stress,” *Chemosphere*, vol. 249, 126341, Jun. 2020.
- [6] H. G. El-Shorbagy, S. M. El-Kousy, K. Z. Elwakeel, and M. A. Abd El-Ghaffar, “Eco-friendly chitosan Condensation adduct resins for removal of toxic silver ions from aqueous medium,” *J. of Ind. Eng. Chem.*, vol. 100, pp. 410–421, Aug. 2021.
- [7] Z. Thong, G. Han, Y. Cui, J. Gao, T. S. Chung, S. Chan, and S. Wei, “Novel nanofiltration membranes consisting of a sulfonated pentablock copolymer rejection layer for heavy metal removal,” *Environ. Sci. Technol.*, vol. 48, pp. 13880–13887, Nov. 2014.
- [8] Y. Mu, Z. Ai, L. Zhang, and F. Song, “Insight into core-shell dependent anoxic Cr(VI) removal with Fe@Fe₂O₃ nanowires: Indispensable role of surface bound Fe(II),” *Appl. Mater. Interfaces*, vol. 7, pp. 1997–2005, Dec. 2014.
- [9] B. Barik, P. S. Nayak, L. S. K. Achary, A. Kumar, and P. Dash, “Synthesis of alumina-based cross-linked chitosan-HPMC biocomposite film: An efficient and user-friendly adsorbent for multipurpose water purification,” *New J. Chem.*, vol. 44, pp. 322–337, Sep. 2019.
- [10] R. Shanmuganathan, T. Edison, F. L. Oscar, P. Kumar, S. Shanmugam, and A. Pugazhendhi, “Chitosan nanopolymers: An overview of drug delivery against cancer,” *Int. J. Biol. Macromol.*, vol. 130, pp. 727–736, Jun. 2019.
- [11] N. M. Crini, E. Lichtfouse, G. Torri, and G. Crini, “Applications of chitosan in food, pharmaceuticals, medicine, cosmetics, agriculture, textiles, pulp and paper, biotechnology, and environmental chemistry,” *Environ. Chem. Lett.*, vol. 17, no. 4, pp. 1667–1692, Jul. 2019.
- [12] T. C. Coutinho, M. C. Ferreira, L. H. Rosa, A. M. de Oliveira, and E. N. de Oliveira, “*Penicillium citrinum* and *Penicillium mallochii*: New phytopathogens of orange fruit and their control using chitosan,” *Carbohydr. Polym.*, vol. 234, 115918, Apr. 2020.
- [13] Y. Shen, J. Z. Guo, L. Q. Bai, X. Q. Chen, and B. Li, “High effective adsorption of Pb(II) from solution by biochar derived from torrefaction of ammonium persulfate pretreated bamboo,” *Bioresour. Technol.*, vol. 323, 124616, Mar. 2021.
- [14] S. Ramola, N. Rawat, A. K. Shankwar, and R. K. Srivastava, “Fixed bed adsorption of Pb and Cu by iron modified bamboo, bagasse and tyre biochar,” *Sustain. Chem. Pharm.*, vol. 22, 100486, Sep. 2021.
- [15] C. Su, Y. Guo, H. Chen, J. Zou, Z. Zeng, and L. Li, “VOCs adsorption of resin-based activated carbon and bamboo char: Porous characterization and nitrogen-doped effect,” *Colloids Surf. A*, vol. 601, 124983, Sep. 2020.
- [16] A. Myers and J. M. Prausnitz, “Thermodynamics of mixed-gas adsorption,” *AIChE*, vol. 11, pp. 121–127, 1965.
- [17] S. B. Ga, S. W. Lee, G. H. Park, J. H. Kim, M. Realf, and J. H. Lee, “New model for S-shaped isotherm data and its application to process modeling using IAST,” *Chem. Eng.*, vol. 420, 127580, Sep. 2021.
- [18] Y. Shao, J. M. Li, X. Y. Fang, Z. Yang, Y. L. Qu, M. Yang, W. Tan, G. Z. Li, and H. B. Wang, “Chemical modification of bamboo activated carbon surface and its adsorption property of simultaneous removal of phosphate and nitrate,” *Chemosphere*, vol. 287, no. 1, 132118, Jan. 2022.
- [19] T. Y. Kim, H. J. Jin, S. S. Park, S. J. Kim, and S. Y. Cho, “Adsorption equilibrium of copper ion and phenol by powdered activated carbon, alginate bead and alginate-activated carbon bead,” *Ind. Eng. Chem.*, vol. 14, pp. 714–719, Nov. 2008.
- [20] S. Babel and T. A. Kurniawan, “Low-cost adsorbents for heavy metals uptake from contaminated water: A review,” *J. Hazard. Mater.*, vol. 97, pp. 219–243, Feb. 2003.
- [21] A. J. F. Garcia, F. J. Beltran, P. Alvarez, and F. J. Masa, “Activated carbon adsorption of some phenolic compounds present in agroindustrial wastewater,” *Adsorption*, vol. 9, pp. 107–115, Jun. 2003.

Copyright © 2024 by the authors. This is an open access article distributed under the Creative Commons Attribution License which permits unrestricted use, distribution, and reproduction in any medium, provided the original work is properly cited ([CC BY 4.0](https://creativecommons.org/licenses/by/4.0/)).